Electronic Supplementary Information

Porphyrin-Poly(arylene ether sulfone)s Covalently Functionalized Multi-Walled Carbon Nanotubes: Synthesis and Enhanced Broadband Nonlinear Optical Properties

Yinlong Du,[a] Ningning Dong,[b] Menghan Zhang,[a] Yunhe Zhang,[a] Jiashuang Luan,[a] Yaning Lu,[a] Shuling Zhang,[a] Ningwei Sun,[a] Jun Wang[b], and Guibin Wang*[a]

[a] College of Chemistry, Key Laboratory of High Performance Plastics, Ministry of Education, Jilin University, Changchun 130012, (P. R. China)
*Prof. Guibin Wang Tel: (+86) 0431 85168889. Fax: (+86) 0431 85168889.
E-mail: wgb@jlu.edu.cn
[b] Key Laboratory of Materials for High-Power Laser, Shanghai Institute of Optics and Fine Mechanics, Chinese Academy of Sciences, Shanghai 201800, (P. R. China)

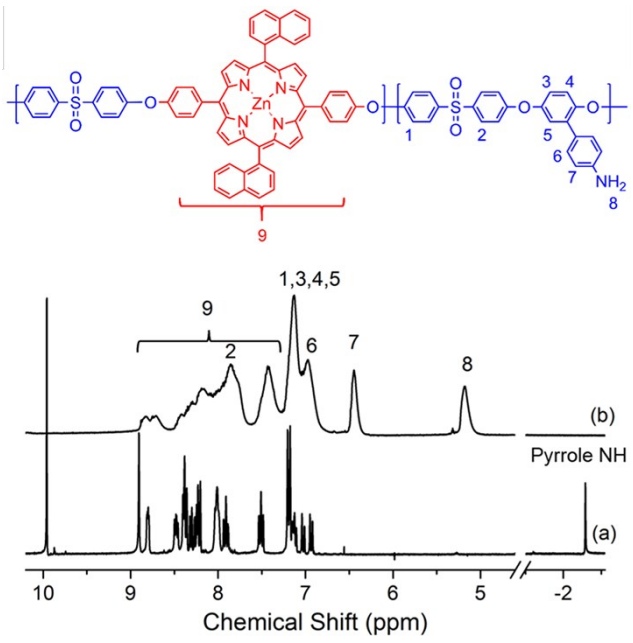

Figure S1. ^{1}H NMR spectrum of (a) porphyrin monomer *trans*-DHTNP and (b) ZnTNP-PAES.

Figure S1 displays the ^{1}H NMR spectrum of ZnTNP-PAES, the signals attributed to protons of porphyrin from 6.9 to 8.8 partially overlaps with those of aromatic protons in the backbones, the characteristic resonance assigned to the internal pyrrole NH proton at -2.80 ppm disappeared after complexation with Zn^{2+}.

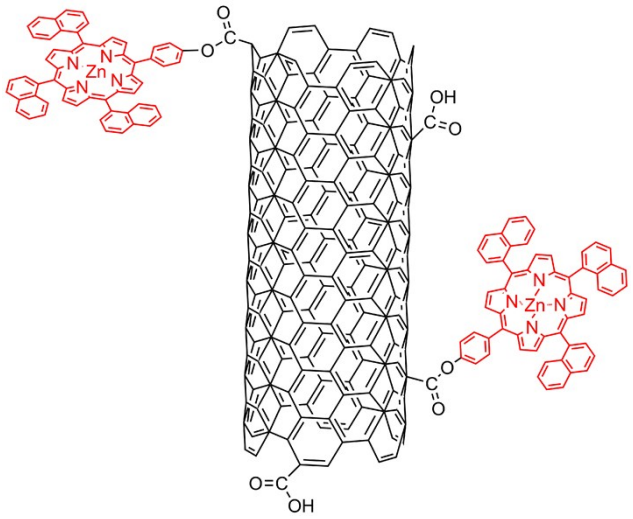

Figure S2. Structure of MWNT-2 hybrid.

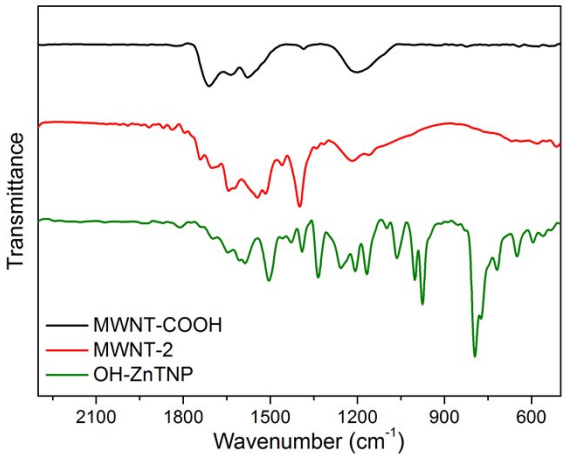

Figure S3. FT-IR spectra of MWNT-2 and OH-ZnTNP.

Figures S2 and **S3** display the structure and IR spectrum of MWNT-2 hybrids. Some characteristic absorption bands of zinc-porphyrins (OH-ZnTNP) are also observed in the region of 1200-1800 cm^{-1}, the weak absorption band at 1744 cm^{-1} is

attributed to the ester bond. These evidence verifies the existence of ZnTNP-PAES and zinc-porphyrins in the MWNT hybrids.

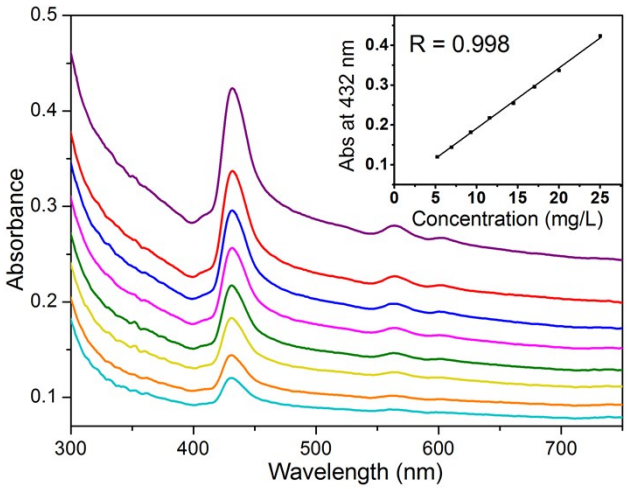

Figure S4. Concentration dependence of the UV-vis absorption spectra of MWNT-1 (concentrations, top to bottom: 25, 20, 17, 14.5, 11.6, 9.2, 6.9, 5.2 mg L^{-1}). Inset: plots of absorption at 431 nm versus concentration.

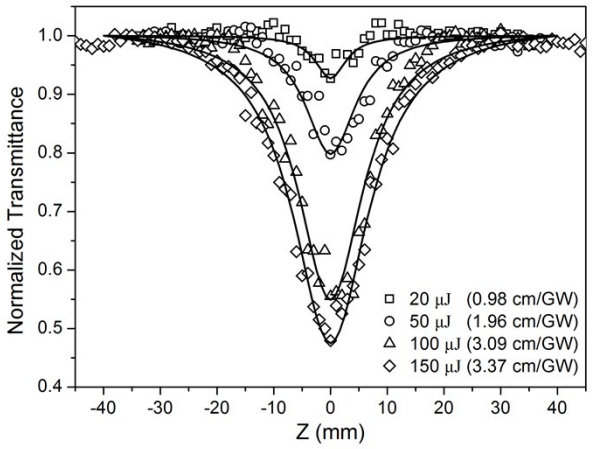

Figure S5. Open-aperture Z-scan curves and β_{eff} values for DMF dispersions of MWNT-1 at 532 nm for different pulse energy.

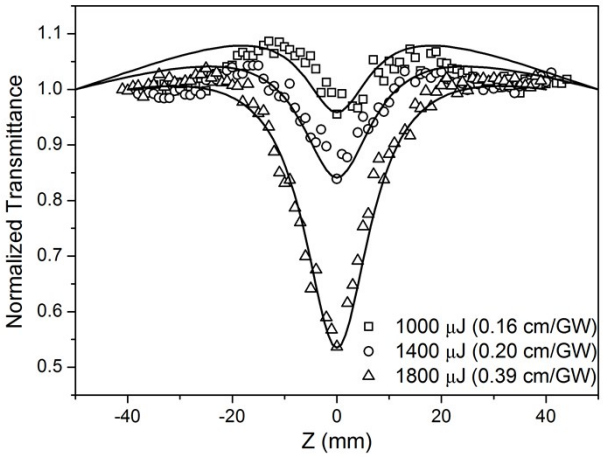

Figure S6. Open-aperture Z-scan curves and β_{eff} values for DMF dispersions of MWNT-1 at 1064 nm for different pulse energy.

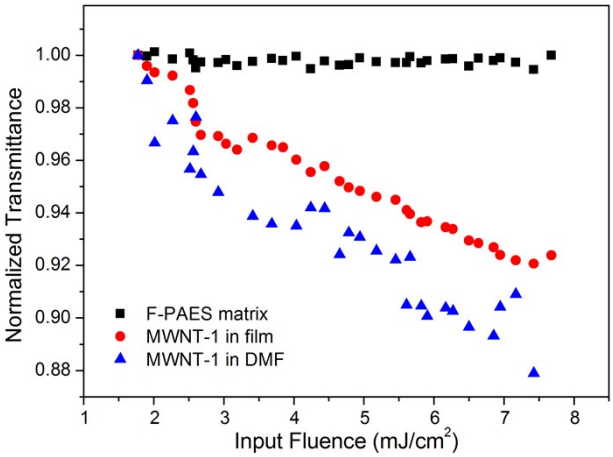

Figure S7. Optical limiting response of MWNT-1 in F-PAES, DMF and neat F-PAES film at 515 nm for 340 fs pulse laser.

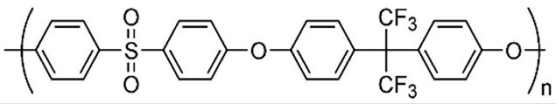

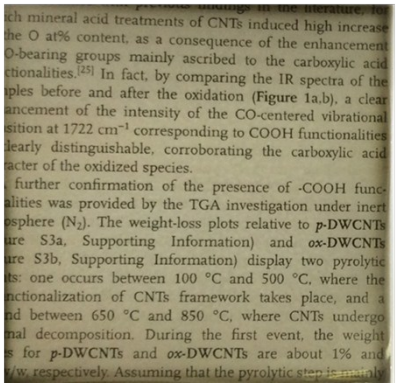
ch mineral acid treatments of CNTs induced high increase
he O at% content, as a consequence of the enhancement
O-bearing groups mainly ascribed to the carboxylic acid
ctionalities.[25] In fact, by comparing the IR spectra of the
ples before and after the oxidation (**Figure** 1a,b), a clear
ancement of the intensity of the CO-centered vibrational
sition at 1722 cm^{-1} corresponding to COOH functionalities
learly distinguishable, corroborating the carboxylic acid
acter of the oxidized species.
further confirmation of the presence of -COOH func-
alities was provided by the TGA investigation under inert
osphere (N_2). The weight-loss plots relative to ***p*-DWCNTs**
ure S3a, Supporting Information) and ***ox*-DWCNTs**
ure S3b, Supporting Information) display two pyrolytic
ts: one occurs between 100 °C and 500 °C, where the
nctionalization of CNTs framework takes place, and a
nd between 650 °C and 850 °C, where CNTs undergo
nal decomposition. During the first event, the weight
s for ***p*-DWCNTs** and ***ox*-DWCNTs** are about 1% and
w/w, respectively. Assuming that the pyrolytic step is mainly

Figure S8. Chemical structure of F-PAES and the photograph of MWNT-1 incorporated F-PAES film.